Simulation of quantum tunnelling on the IBM quantum computers

Author: Berta Martínez Pàmias.

Facultat de Física, Universitat de Barcelona, Diagonal 645, 08028 Barcelona, Spain.[*]

Advisor: Bruno Juliá Díaz

Abstract: We study the time evolution of a particle in a double-well potential using IBM quantum computers and a classical computer. Firstly, we go over the methods for the numerical simulation and the quantum computer implementation. As an example, we simulate the system in a 4-point space using 2-qubit circuits. Finally, we compare the results obtained with the different methods and discuss their dissimilarities and sources of error.

I. INTRODUCTION

Quantum simulation in quantum computers has advantages for large systems over numerical simulation in classical computers. Quantum computers allow more information to be stored with fewer resources, which is useful due to the rapidly increasing dimension of Hilbert space in quantum systems. For this reason, quantum simulation has been widely studied in recent years.

In this work, we will use the digital quantum simulation method proposed by A.T. Sornborger [1] for small systems, which does not require ancillary qubits to implement the operators and needs few gates per time step. Due to the small size of the simulated system, it is possible to compare the results from the quantum simulation with a numerical simulation. The simulated system will be a particle in a double-well. Thence, quantum tunneling, which is a purely quantum effect, will be observed.

To carry out the project, we use the open-access devices from the IBM Quantum Experience [2]. IBM provides access to both classical systems to simulate a quantum computer, and also to actual quantum computers.

In section II, the theoretical background of the methods is explained and afterwards, in section III, the methods and their implementation in the corresponding device are described. Finally, the results are presented and discussed in section IV.

II. THEORETICAL BACKGROUND

The Schrödinger equation in one dimension for a single particle with a time-independent Hamiltonian is

$$i\hbar \frac{\partial \Psi(x,t)}{\partial t} = \hat{H}\Psi(x,t), \tag{1}$$

where the Hamiltonian has a potential and a kinetic part, $(\hat{H} = \hat{V} + \hat{K})$. They can be expressed as $\hat{V} = V(x)$ and $\hat{K} = \frac{\hat{p}^2}{2m}$, respectively. For simplicity, Eq. (1) has been adimensionalized with $\hbar = 1$ and $m = \frac{1}{2}$, and from now

on everything is dimensionless and has no units. Then, the time evolution of the wave function is

$$\Psi(x, t + \Delta t) = e^{-i\hat{H}\Delta t}\Psi(x,t) = e^{-i(\hat{V}+\hat{K})\Delta t}\Psi(x,t). \tag{2}$$

Even though the two operators do not usually commute, the exponential from Eq. (2) can be split using the first-order Suzuki-Trotter decomposition ($e^{i(A+B)\Delta t} = e^{iA\Delta t}e^{iB\Delta t} + \mathcal{O}(\Delta t^2)$), if Δt is small enough [3],

$$\Psi(x, t + \Delta t) \approx [e^{-i\hat{V}\Delta t}e^{-i\hat{K}\Delta t} + \mathcal{O}(\Delta t^2)]\Psi(x,t). \tag{3}$$

The potential operator is diagonal in the coordinate space and the kinetic operator in the momentum space. The latter is useful to use Eq. (3) in practice,

$$\langle x|\Psi(\Delta t)\rangle = \langle x| e^{-i\hat{V}\Delta t} \sum_p |p\rangle \langle p| e^{-i\hat{K}\Delta t} \sum_{x'} |x'\rangle \langle x'|\Psi(0)\rangle$$

$$= e^{-i\hat{V}\Delta t} \sum_p \langle x|p\rangle e^{-i\hat{K}\Delta t} \sum_{x'} \langle p|x'\rangle \langle x'|\Psi(0)\rangle$$

$$= e^{-i\hat{V}\Delta t} \, \mathrm{F}^\dagger e^{-i\hat{K}\Delta t} \, \mathrm{F} \, \langle x'|\Psi(0)\rangle, \tag{4}$$

where we have introduced the resolution of the identity and $\langle x|p\rangle = \frac{1}{\sqrt{2\pi}}e^{ipx}$, to obtain the Fourier transform and its inverse.

III. METHODS

A. Numerical implementation

The numerical simulation of the time evolution of a system can be implemented in a classical computer with the following steps:

1. Define the problem parameters such as space dimension and time steps.

2. Discretize the space coordinate in an equally spaced grid, $x_k = x_0 + k\Delta x$.

3. Consider the corresponding discreet momenta. To make sure it has positive and negative values, it can be defined as (proposed by [4] and [5])

$$\begin{cases} p_j = \frac{2\pi}{x_{\dim}}j & 0 \leq j \leq \frac{x_{\dim}}{2} \\ p_j = \frac{2\pi}{x_{\dim}}\left(\frac{x_{\dim}}{2} - j\right) & \frac{x_{\dim}}{2} < j < x_{\dim} \end{cases}. \tag{5}$$

---

[*]Electronic address: `bmartipa56@alumnes.ub.edu`

4. Discretize the whole time interval into small enough steps $\Delta t = \frac{t_{\max} - t_{\min}}{t_{\text{steps}} - 1}$.

5. Define the initial wave function $\Psi(x, t_{\min})$ for every point in the coordinate space.

6. Time evolution. Iterate t_{steps} times:

(a) Implement a Fourier transform from x-space to p-space acting on $\Psi(x, 0)$,

$$\tilde{\Psi}(p_j, 0) = \frac{1}{\sqrt{2\pi}} \sum_{k=1}^{x_{\dim}} e^{-ip_j x_k} \Psi(x_k, 0) \Delta x. \qquad (6)$$

(b) Implement the kinetic operator acting on $\tilde{\Psi}(p, 0)$,

$$\tilde{\Phi}(p_j, 0) = e^{-ip_j^2 \Delta t} \tilde{\Psi}(p_j, 0). \qquad (7)$$

(c) Implement a Fourier transform to come back to x-space,

$$\Phi(x_k, 0) = \frac{1}{\sqrt{2\pi}} \sum_{j=1}^{x_{\dim}} e^{ip_j x_k} \tilde{\Phi}(p_j, 0) \Delta p. \qquad (8)$$

(d) Implement the potential operator and finally obtain $\Psi(x, \Delta t)$,

$$\Psi(x_k, \Delta t) = e^{-iV(x_k)\Delta t} \Phi(x_k, 0). \qquad (9)$$

(e) Repeat the process with $\Psi(x, \Delta t)$ as the initial wave function.

7. After t_{steps}, we have obtained $\Psi(x, t_{\max})$ and its probability density, $|\Psi(x_k, t)|^2 = \Psi^*(x_k, t)\Psi(x_k, t)$.

1. Example: Free Gaussian

This method allows to obtain the time evolution of any system with an arbitrary space dimension and length. As an example, the results of a numerical simulation for a free Gaussian wave packet are shown in Fig. 1, where the spreading of the wave packet with time is clearly seen. The numerical simulation is compared to the analytical solution, showing a very good agreement.

B. Quantum computer implementation

The time evolution can be achieved on a quantum computer through the implementation of different gates. In this case, the size of the space (N) is given by the number of qubits used (n): $N = 2^n$. In this work, as an academic example and following Ref. [1], only 2 qubits have been used. Therefore, we have a lattice of 4 points defined by the following states: $|00\rangle, |01\rangle, |10\rangle$ and $|11\rangle$.
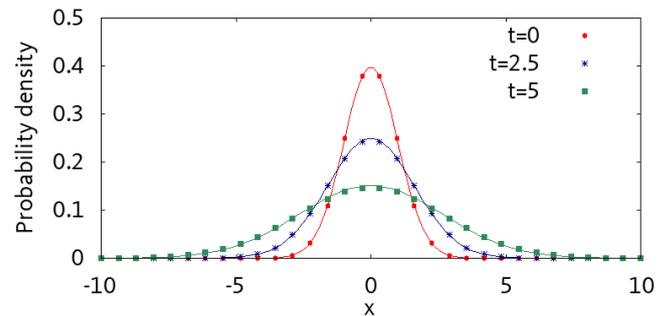

FIG. 1: Time evolution of a free Gaussian wave packet in a space of 32 points and $-10 < x < 10$. The numerical simulation (dots) and the analytical results (lines) are shown for three different times.

1. Potential operator

The potential can be introduced to the system by rotating the state of a certain qubit, as it is proposed in [1]. To do so, the single-qubit Z-Rotation gate can be used. In a circuit with 2 qubits, the Z-Rotation gate must be implemented on the lowest order qubit (q_0) to obtain a double-well potential,

$$e^{-iV\Delta t} = I \otimes e^{-iv\sigma_z \Delta t} = \begin{pmatrix} e^{-iv\Delta t} & 0 & 0 & 0 \\ 0 & e^{iv\Delta t} & 0 & 0 \\ 0 & 0 & e^{-iv\Delta t} & 0 \\ 0 & 0 & 0 & e^{iv\Delta t} \end{pmatrix}, \qquad (10)$$

where v is the parameter that characterizes the height of the potential. If we would like to obtain a step potential, the Z-Rotation gate should be applied to the highest order qubit (q_1). On the IBM quantum computers, it can be done using the RZ(λ) gate with $\lambda = 2v\Delta t$,

$$\text{RZ}(\lambda) = \begin{pmatrix} e^{-i\frac{\lambda}{2}} & 0 \\ 0 & e^{i\frac{\lambda}{2}} \end{pmatrix}. \qquad (11)$$

2. Quantum Fourier Transform

The Quantum Fourier Transform (QFT) can be expressed for an arbitrary number of qubits as [6],

$$|j\rangle \to \frac{1}{\sqrt{N}} \sum_{k=0}^{N-1} e^{\frac{2\pi ijk}{N}} |k\rangle. \qquad (12)$$

Developing Eq. (12) for 2 qubits (n=2, hence N=4):

$$\text{QFT} |j_1 \, j_2\rangle = \frac{1}{2} \left[\left(|0\rangle + e^{2\pi i \frac{j_2}{2}} |1\rangle \right) \otimes \left(|0\rangle + e^{2\pi i (\frac{j_1}{2} + \frac{j_2}{2^2})} |1\rangle \right) \right]. \qquad (13)$$

On IBM, j_1 corresponds to q_1 and j_2 to q_0. To implement the QFT we use Hadamard and controlled-phase gates:
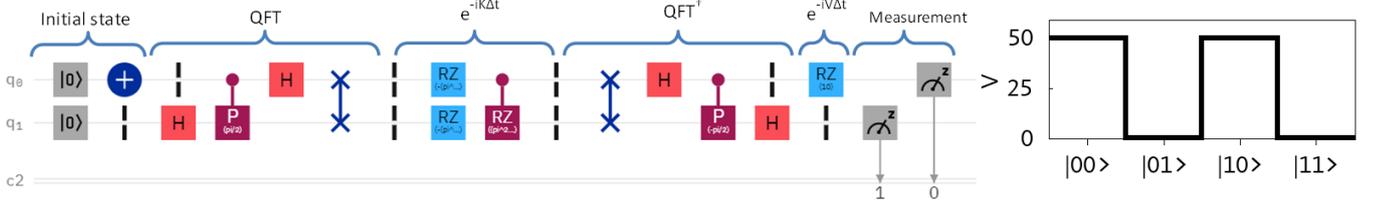
FIG. 2: On the left, circuit for a single time step of the time evolution of a particle initially at $|01\rangle$ in a double-well potential with barriers ($v = 50$) at $|00\rangle$ and $|10\rangle$ and $\Delta t = 0.1$. Image obtained from the circuit composer in [2]. On the right, the 4-point space and the potential produced by the circuit, are displayed.

1. First of all, a Hadamard gate is applied to the highest order qubit,

$$H |j_1\rangle \otimes |j_2\rangle = \frac{1}{\sqrt{2}} \big(|0\rangle + e^{2\pi i \frac{j_1}{2}} |1\rangle \big) \otimes |j_2\rangle . \quad (14)$$

2. A controlled-phase gate is implemented to both qubits with the control on the lowest order qubit,

$$\begin{aligned} &R_2\Big(\frac{1}{\sqrt{2}} \big(|0\rangle + e^{2\pi i \frac{j_1}{2}} |1\rangle \big) \otimes |j_2\rangle \Big) \\ &= \frac{1}{\sqrt{2}} \big(|0\rangle + e^{2\pi i (\frac{j_1}{2} + \frac{j_2}{2^2})} |1\rangle \big) \otimes |j_2\rangle . \end{aligned} \quad (15)$$

Where $R_k = \begin{pmatrix} 1 & 0 \\ 0 & e^{\frac{2\pi i}{2^k}} \end{pmatrix}$ and it can be applied on IBM with the phase gate $P(\lambda) = \begin{pmatrix} 1 & 0 \\ 0 & e^{i\lambda} \end{pmatrix}$ with $\lambda = \frac{\pi}{2}$.

3. Another Hadamard gate is implemented to the lowest order qubit,

$$\begin{aligned} &\frac{1}{\sqrt{2}} \big(|0\rangle + e^{2\pi i (\frac{j_1}{2} + \frac{j_2}{2^2})} |1\rangle \big) \otimes H |j_2\rangle \\ &= \frac{1}{\sqrt{2}} \big(|0\rangle + e^{2\pi i (\frac{j_1}{2} + \frac{j_2}{2^2})} |1\rangle \big) \otimes \frac{1}{\sqrt{2}} \big(|0\rangle + e^{2\pi i \frac{j_2}{2}} |1\rangle \big) . \end{aligned} \quad (16)$$

4. To obtain the same expression as in Eq. (13), one needs to swap the order of the qubits,

$$\begin{aligned} &\text{SWAP } \frac{1}{2} \Big[\big(|0\rangle + e^{2\pi i (\frac{j_1}{2} + \frac{j_2}{2^2})} |1\rangle \big) \otimes \big(|0\rangle + e^{2\pi i \frac{j_2}{2}} |1\rangle \big) \Big] \\ &= \frac{1}{2} \Big[\big(|0\rangle + e^{2\pi i \frac{j_2}{2}} |1\rangle \big) \otimes (|0\rangle + e^{2\pi i (\frac{j_1}{2} + \frac{j_2}{2^2})} |1\rangle) \Big] . \end{aligned} \quad (17)$$

3. Kinetic operator

The kinetic operator can be implemented in the momentum space thanks to the QFT. In this space, the operator is diagonal with the momentum values in the diagonal elements. It can be implemented as proposed by [1]:

$$e^{-iK\Delta t} = \exp\left[-i\Big(\frac{-2\pi}{4}\Big)^2 \begin{pmatrix} 0 & 0 & 0 & 0 \\ 0 & 4 & 0 & 0 \\ 0 & 0 & 1 & 0 \\ 0 & 0 & 0 & 1 \end{pmatrix} \Delta t \right] = \Phi_{01} Z_1 Z_0 . \quad (18)$$

The first gate in Eq. (18) is

$$\Phi_{01} = \exp\left[-i\gamma c_2 \begin{pmatrix} 1 & 0 & 0 & 0 \\ 0 & 1 & 0 & 0 \\ 0 & 0 & 1 & 0 \\ 0 & 0 & 0 & -1 \end{pmatrix} \Delta t \right] . \quad (19)$$

This matrix can be applied with the previously presented $RZ(\lambda)$ gate on q_1 with a control on q_0, where $\lambda = 2\gamma c_2 \Delta t = \pi^2 \Delta t$,

$$C - RZ(\lambda) = \begin{pmatrix} e^{-i\frac{\lambda}{2}} & 0 & 0 & 0 \\ 0 & e^{-i\frac{\lambda}{2}} & 0 & 0 \\ 0 & 0 & e^{-i\frac{\lambda}{2}} & 0 \\ 0 & 0 & 0 & e^{i\frac{\lambda}{2}} \end{pmatrix} . \quad (20)$$

The other two gates in Eq. (18) are single-qubit gates implemented on each qubit,

$$Z_1 = e^{-i\gamma c_1 \sigma_z \Delta t} \otimes I = \begin{pmatrix} e^{-i\gamma c_1 \Delta t} & 0 \\ 0 & e^{i\gamma c_1 \Delta t} \end{pmatrix} \otimes I , \quad (21)$$

$$Z_0 = I \otimes e^{-i\gamma c_0 \sigma_z \Delta t} = I \otimes \begin{pmatrix} e^{-i\gamma c_0 \Delta t} & 0 \\ 0 & e^{i\gamma c_0 \Delta t} \end{pmatrix} . \quad (22)$$

Both can be carried out with the $RZ(\lambda)$ gate. Z_1 must be applied to qubit q_1 with $\lambda = 2\gamma c_1 \Delta t = -\pi^2 \Delta t$ and Z_0 to q_0 with $\lambda = 2\gamma c_0 \Delta t = -\frac{\pi^2}{4} \Delta t$. The coefficients obtained by [1] are $c_0 = -1$, $c_1 = -4$, $c_2 = 4$ and $\gamma = \big(-\frac{2\pi}{4} \big)^2 \frac{1}{\sqrt{4}}$.

4. Quantum circuit

Applying all the aforementioned gates, one obtains the time evolution circuit for a single time step shown in Fig. 2. To acquire the evolution for a time t with an interval
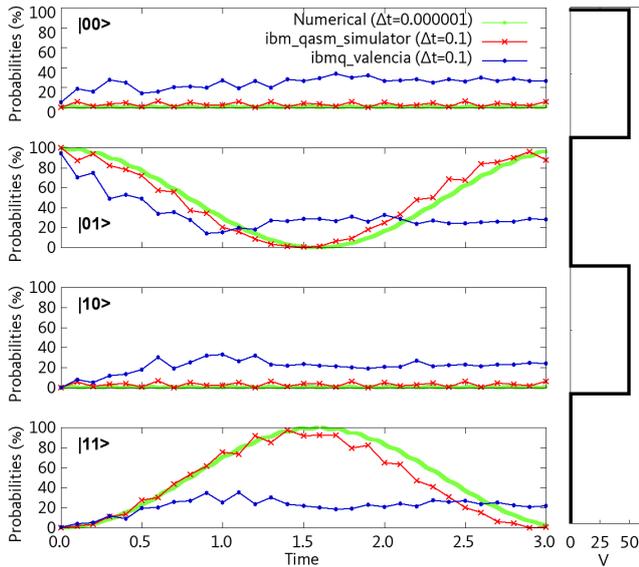
FIG. 3: Time evolution of a particle initially at $|01\rangle$ in a double-well potential with barriers ($v = 50$) at $|00\rangle$ and $|10\rangle$. Results obtained numerically (with $\Delta t = 0.000001$), with the ibmq_qasm_simulator ($\Delta t = 0.1$) and with the 5-qubit quantum computer ibmq_valencia ($\Delta t = 0.1$). The shape of the potential is shown on the right.

Δt, it is necessary to run a circuit with n time steps so that $t = n\Delta t$. Thus, to obtain the results for every instant until t, n circuits should be ran (each with its own number of time steps). This procedure implies that the larger the time we want to achieve, the larger the circuit and more circuits are required to get the results at every time step.

IV. RESULTS

In this section, the results for a 4-point system obtained from the methods from section III, are presented. All results from the IBM's quantum computers and simulator have been achieved with 8192 shots (number of repetitions of a measurement).

A. Double-well potential

When a particle is set in one of the wells of a double-well potential, it tunnels through the barrier into the other well. This can be observed in Fig. 3, where a particle initially at $|01\rangle$ passes to $|11\rangle$ and comes back to the initial state. The period of this oscillation is $T \approx 3$.

The results from the numerical simulation can be taken as a reference since its Δt is small enough to dismiss the error produced by the discretization of time. The differences between these results and the ones from the IBM's quantum simulator (ibmq_qasm_simulator) come from the different Δt used and the dissimilarities in both
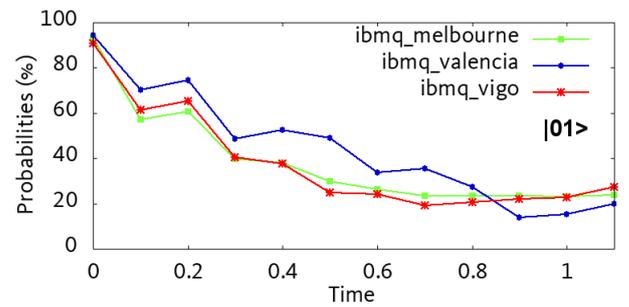

FIG. 4: Time evolution of state $|01\rangle$ of a system with a particle initially at $|01\rangle$ in a double-well potential with barriers ($v = 50$) at $|00\rangle$ and $|10\rangle$. Results obtained with 5-qubit quantum computers ibmq_valencia and ibmq_vigo, and 15-qubit computer ibmq_melbourne. All the results have $\Delta t = 0.1$.

methods. While the numerical results come from a numerical computation, the results from the simulator are obtained through sampling.

The results running in the quantum computer (ibmq_valencia) show the correct trend for very short times, $t \leq 0.5$. Above that, the results are clearly different from the expected ones, i.e. the tunneling is no longer observed. The reason for this disagreement, is that the implementation of gates in a real quantum device has an associated error, which becomes more important for bigger times (more time steps require more gates). There is also a readout error when measurements are performed.

Another important issue that occurs in the quantum computer is quantum decoherence. When the running time of a circuit exceeds the coherence time of the qubits, the system does not show a quantum behaviour anymore and the results are not useful. Observing Fig. 3, it can be deduced that quantum decoherence happens approximately around the running time of a 10 time steps circuit.

1. Comparison of the results of different quantum computers

As it has been mentioned before, the implementation of a circuit in a quantum computer has some associated errors. These errors depend on the gates and the qubits of each computer. Thus, as it can be seen in Fig. 4, the results obtained for different devices differ from one another due to their own sources of errors. It can also be seen that in all cases, the initial state does not have a 100% probability as a consequence of the devices' noise.

2. Comparison of the results with different Δt

The discretization of time due to Suzuki-Trotter decomposition in Eq. (3) produces an error that scales as $\mathcal{O}(\Delta t^2)$. To minimize this error one should work with the lowest possible Δt. This is plausible for the numer-
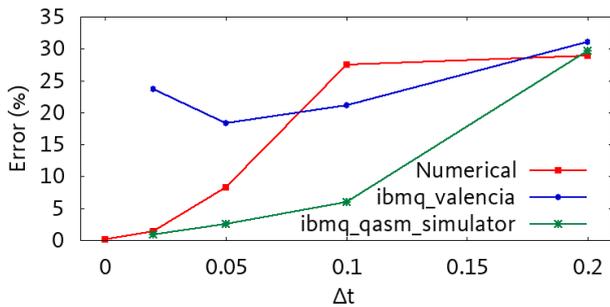
FIG. 5: Root mean squared errors per time step for different Δt in the numerical simulation, the ibm_qasm_simulator and the 5-qubit quantum computer ibmq_valencia. The errors have been obtained comparing the results for every Δt with the numerical results for $\Delta t = 0.000001$. Results correspond to the time evolution of a particle initially at $|01\rangle$ in a double-well potential with barriers ($v = 50$) at $|00\rangle$ and $|10\rangle$.
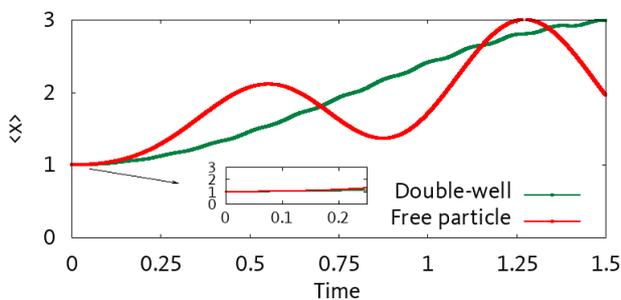

FIG. 6: Expected x values of the time evolution of a free particle and a particle in a double-well. Both results have been acquired with the numerical simulation using $\Delta t = 0.000001$. The inset shows a close-up view of the initial instants. ($x = 0$ represents state $|00\rangle$, $x = 1$ is state $|01\rangle$ and so on.)

ical simulation, but in the IBM's simulator and quantum computer, reducing Δt implies that more gates are required to achieve a certain time. Therefore, the accumulated gate error becomes bigger (in the quantum computer case). It also increases the running time, which can exceed the coherence time of the qubits and produce unuseful results as mentioned previously. It is necessary to use a Δt small enough to reduce its error, but big enough to be able to achieve some time evolution.

In Fig. 5, it is observed that for smaller Δt, the error becomes lower. In the quantum computer case, the noise

from the device does not allow to obtain errors as low as in the numerical simulation or the simulator. It can be seen as well, that the error reduces faster in the simulator than in the numerical computation. This disparities probably come from the differences between methods.

B.   Free particle

If we now set $v = 0$, a free particle is obtained. Comparing it with the double-well potential results, it can be seen how the potential operator effects the system.

While for the particle in a double-well we observe how it smoothly passes from one well to the other, for a free particle it is first observed an equally spreading through the space, which maintains $\langle x \rangle$ constant (as shown on the inset of Fig. 6). Since the space is really small, the particle rapidly encounters the limits of the space and bounces back. This creates phenomena such as interference. Because the initial position of the particle is not centered, it first encounters the lower limit of the space, which gives an impulse to the particle that makes it stay in the superior part of the space.

V.   CONCLUSIONS

In this work, we have solved the dynamics of a single particle in presence of an external potential by means of classical algorithms and quantum algorithms implemented in both quantum simulators and IBM quantum computers. We have used the digital quantum particle simulation proposed in Ref. [1] and numerical computation to simulate a particle in a double-well potential.

The obtained results with the IBM devices have been compared with the numerical results. We have seen that, even in small simulations such as this one, where the space is discretized to just four points, the errors inherent to the quantum computer implementation are still large for practical uses.

[1] Sornborger, A.T. "Quantum Simulation of Tunneling in Small Systems". Sci. Rep. **2**: 597 (2012).
[2] IBM. *IBM Quantum Experience*. https://quantum-computing.ibm.com (2016).
[3] Zalka, C. "Simulating Quantum Systems on a Quantum Computer". Proc. R. Soc. Lond. A. **454**: 313-322 (1998).
[4] Hegade, N.N. *et al.* "Experimental Demonstration of Quantum Tunneling in IBM Quantum Computer". arXiv:1712.07326 (2017).
[5] Feng, G. *et al.* "Experimental simulation of quantum tunneling in small systems". Sci. Rep. **3**: 2232 (2013).
[6] Nielsen, M. and Chuang, I. *Quantum Computation and Quantum Information*, (Cambridge University Press, Cambridge 2010, 10th Anniversary Ed.).